Int. J. Heat Mass Transfer. Vol. 36, No. 6, pp. 1459–1469, 1993
Printed in Great Britain

0017-9310/93 $6.00 + 0.00

Turbulent flow in a channel with transverse rib heat transfer augmentation

B. H. CHANG and A. F. MILLS
School of Engineering and Applied Science, University of California, Los Angeles, CA 90024-1597, U.S.A.

(*Received* 24 *June* 1992 *and in final form* 10 *August* 1992)

Abstract—Turbulent flow in a two-dimensional channel with repeated rectangular rib roughness was numerically simulated using a low Reynolds number form of the k–ε turbulence model. Friction factors and average Stanton numbers were calculated for various pitch to rib height ratios and bulk Reynolds numbers. Comparisons with experiment were generally adequate, with the predictions of friction superior to those for heat transfer. The effect of variable properties for channel flow was investigated, and the results showed a greater effect for friction than for heat transfer. Comparison with experiment yielded no clear conclusions. The turbulence model was also validated for a related problem, that of flow downstream of an abrupt pipe expansion.

INTRODUCTION

ENHANCED surfaces are used to increase the convective heat transfer coefficient for high heat flux applications. The use of parallel rectangular ribs at an optimal spacing has been explored for applications such as gas-cooled nuclear reactors [1, 2] and gas turbine blades [3, 4]. Current interest in hypersonic flight has led to renewed activity in the design of structures that can accommodate high heat fluxes and withstand high temperatures. A promising approach for hydrogen fueled vehicles is to use cooling panels through which supercritical hydrogen is pumped before injection into the engine. Figures 1(a) and (b) show a possible cooling panel design for use in a scramjet inlet. Although much experimental data has been obtained for the effects of repeated rib roughness on friction and heat transfer, little has been accomplished analytically or numerically. Thus current engineering practice is to use empirically determined roughness functions to describe the near wall region, and analytical or numerical solution schemes to calculate the core flow. A major difficulty in applying this technique to the flow of supercritical hydrogen in cooling panels is the large thermophysical property variations that characterize the flow. These variations arise both due to the large wall to bulk temperature ratios encountered, and also to the peculiar nature of the property variations near the critical point. No reference property or similar scheme is available for accounting for these variable property effects, and no experimental data base exists for supercritical hydrogen flow over repeated rib roughness.

The first attempt to analytically determine the roughness functions for flow over rectangular ribs was made by Lewis [5]. The flow was approximated by a series of attached and separated flow regions, and some empirical information from experiments over cavities and steps was required. The k–ε turbulence model with the wall function boundary condition was used by Lee *et al.* [6] to predict roughness functions in an annulus with ring type rectangular roughness on the inner pipe. In a numerical study, fully developed flow in a single module was solved using the periodicity conditions, as proposed by Patankar *et al.* [7], in order to avoid the entrance region problem. A correction to the turbulent viscosity similar to that of Leschziner and Rodi [8] was used to account for extra strain rates due to streamline curvature. Liou *et al.* [9] made numerical computations for turbulent flow over a single rib roughness in a channel. Numerical calculations for flow over two rib roughnesses in a channel were performed by Durst *et al.* [10] and Liou *et al.* [11]. Standard wall functions were used in all these numerical studies.

Use of wall functions as boundary conditions when solving turbulent flows using the k–ε model has been relatively successful where properties are constant. But for large and irregular property variations in the viscous sublayer and buffer layers, the use of wall functions presents a fundamental problem. One

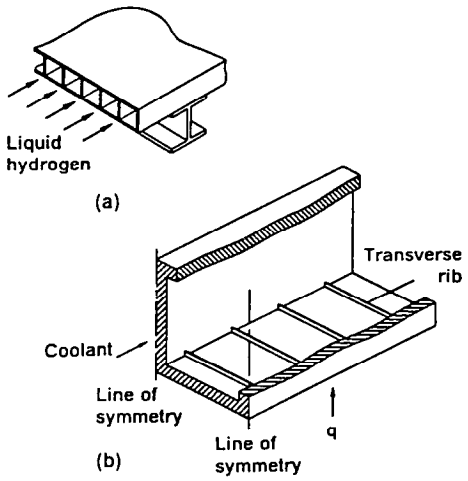

FIG. 1. (a) A cooling panel. (b) Repeated ribs to augment heat transfer.

NOMENCLATURE

b width of roughness
$c_\mu, c_{\varepsilon 1}, c_{\varepsilon 2}$ turbulence model constants
c_l coefficient in source term of dissipation rate equation
c_p constant pressure specific heat
d upstream tube diameter
D downstream tube diameter
D_h hydraulic diameter
e roughness height, or $(D-d)/2$
f friction factor
f_μ, f_ε empirical functions in turbulence model
h enthalpy
H half of the channel height
k turbulence kinetic energy, $\frac{1}{2}\overline{u_i' u_i'}$
L rib pitch
Nu Nusselt number based on downstream diameter
p pressure
Pr molecular Prandtl number
Pr_t turbulent Prandtl number
Re Reynolds number
St Stanton number
U streamwise mean velocity
u' streamwise velocity fluctuation
V lateral mean velocity
$\tilde{V}$ mass averaged lateral velocity
v' lateral velocity fluctuation
w rib width
x axial distance
y normal distance from the wall.

Greek symbols
Γ thermal conductivity
ε turbulence dissipation rate
$\tilde{\varepsilon}$ modified dissipation variable
μ dynamic viscosity
μ_t turbulent viscosity
ν kinematic viscosity
ν_t turbulent kinematic viscosity
ρ density
σ_ϕ turbulent Prandtl number for ϕ, $\phi = k, \varepsilon, h$.

Subscripts
av average
b bulk
c constant property
w wall.

approach would be to use a reference property scheme in the wall functions. However, one could then argue that it would be simpler and more direct to have a reference property scheme for the transfer coefficients themselves. Also, the highly irregular property variations near the critical point of hydrogen complicates the development of reference property schemes. An alternative approach is to integrate the transport equations to the wall using exact thermophysical properties and thus avoid the use of wall functions. In an earlier study [12] we used this approach for constant property flow in a rib roughened circular tube. Here we turn attention to two-dimensional channel flow with transverse ribs and present results for both constant property and variable property flows. With a numerical solution procedure it is relatively simple to allow for property variations exactly, and hence to study the effects of these parametrically. In addition, once the solution procedure has been validated, it is relatively simple to vary key geometrical parameters, such as rib pitch, height and shape. A suitable turbulence model was chosen by examining a simpler related problem, namely, the abrupt pipe expansion, with its characteristic flow reattachment and recirculation region. This problem has received considerable attention both in experimental and numerical studies. Recently Yap [13] has made a thorough numerical study using various turbulence models. The best heat transfer prediction was obtained with a low-Reynolds number k–ε turbulence model across the viscous sublayer and an algebraic stress model in core. However, the Jones and Launder version of the low-Reynolds number k–ε model [14] employed for the whole flow regime gave fairly good predictions, provided an appropriate source term was added to the transport equation for the turbulence dissipation rate. Yap also found that the wall function approach showed poor Reynolds number dependence for the peak Nusselt number, even with the algebraic stress model employed in core. Though not presented in this study, the abrupt pipe expansion flow was investigated using wall functions. It was found that the non-dimensional viscous sublayer thickness had to be related to the near-wall turbulence level, as in the method of Ciofalo and Collins [15], in order to improve heat transfer prediction for flows with reattachment. The wall function method performed poorly in general, especially for a small step height or low Reynolds number, since insufficient grids could be employed to resolve the flow below the step. The Yap modified Jones and Launder model was used for the current study.

ANALYSIS

Mean transport equations

The set of elliptic partial differential equations governing mass, momentum, and energy conservation for a steady incompressible flow are written as follows:

$$\frac{\partial}{\partial x_i}(\rho U_i) = 0 \tag{1}$$

$$\frac{\partial}{\partial x_j}(\rho U_i U_j) = -\frac{\partial P}{\partial x_j} + \frac{\partial}{\partial x_j}\left[\mu\left(\frac{\partial U_i}{\partial x_j} + \frac{\partial U_j}{\partial x_i}\right) - \rho\overline{u_i' u_j'}\right] \tag{2}$$

$$\frac{\partial}{\partial x_j}(\rho U_j h) = \frac{\partial}{\partial x_j}\left[\Gamma\frac{\partial}{\partial x_j}\left(\frac{h}{c_p}\right) - \rho\overline{u_j' h'}\right]. \tag{3}$$

The time mean of the product of the fluctuating velocities are modeled using the modified Boussinesq concept,

$$-\overline{u_i' u_j'} = \nu_t\left(\frac{\partial U_i}{\partial x_j} + \frac{\partial U_j}{\partial x_i}\right) - \tfrac{2}{3}k\delta_{ij}. \tag{4}$$

The turbulent heat flux is similarly modeled by introducing the turbulent Prandtl number,

$$-\rho\overline{u_j' h'} = \frac{\mu_t}{Pr_t}\frac{\partial h}{\partial x_j}. \tag{5}$$

The assumptions employed in the governing equations for variable property flow are that the product of the average quantity ρU is much greater than $\overline{\rho' u'}$, and a new normal velocity $\tilde{V}$ is defined as $\rho\tilde{V} = \rho V + \overline{\rho' v'}$, since $\overline{\rho' v'}$ can be of the same order of magnitude as ρV in low-speed flows with heating [16]. Other terms involving density fluctuation have been neglected, since $\rho'/\bar{\rho}$ is expected to be fairly small.

Turbulence model

The Jones and Launder low Reynolds number turbulence model, with some constants modified by Launder and Sharma [17] is used for the computations. The turbulence kinetic energy, k, and the modified dissipation variable, $\tilde{\varepsilon}$, are obtained from the following transport equations:

$$\frac{\partial}{\partial x_j}(\rho U_j k) = \frac{\partial}{\partial x_j}\left[\left(\frac{\mu_t}{\sigma_k} + \mu\right)\frac{\partial k}{\partial x_j}\right] - \rho\overline{u_i' u_j'}\frac{\partial U_i}{\partial x_j} - \rho\tilde{\varepsilon} - 2\mu\left(\frac{\partial k^{1/2}}{\partial x_k}\right)^2 \tag{6}$$

$$\frac{\partial}{\partial x_j}(\rho U_j\tilde{\varepsilon}) = \frac{\partial}{\partial x_j}\left[\left(\frac{\mu_t}{\sigma_\varepsilon} + \mu\right)\frac{\partial\tilde{\varepsilon}}{\partial x_j}\right] - c_{\varepsilon 1}\rho\frac{\tilde{\varepsilon}}{k}\overline{u_i' u_j'}\frac{\partial U_i}{\partial x_j} - c_{\varepsilon 2}f_\varepsilon\rho\frac{\tilde{\varepsilon}^2}{k} + \frac{2\mu\mu_t}{\rho}\left(\frac{\partial^2 U_i}{\partial x_k^2}\right)^2. \tag{7}$$

The turbulent viscosity, μ_t, is given by

$$\mu_t = c_\mu f_\mu\rho\frac{k^2}{\tilde{\varepsilon}} \tag{8}$$

where the dissipation rate, ε, is equal to $\tilde{\varepsilon} + 2\nu(\partial k^{1/2}/\partial x_k)^2$. The empirical coefficients adopted are

$$f_\mu = \exp\left[\frac{-3.4}{(1+Re_t/50)^2}\right]$$

$$f_\varepsilon = 1.0 - 0.3\exp(-Re_t^2)$$

$$Re_t = \frac{k^2}{\nu\tilde{\varepsilon}}$$

$$c_\mu = 0.09, \quad c_{\varepsilon 1} = 1.44, \quad c_{\varepsilon 2} = 1.92,$$

$$\sigma_\varepsilon = 1.3, \quad \sigma_k = 1.0. \tag{9}$$

Yap [13] calculated the flow for an abrupt pipe expansion using the k–ε turbulence model, and found that the predicted heat transfer rates in the vicinity of the reattachment point some 5 times higher than experimental values. Yap observed that the cause of this discrepancy was a predicted length scale that was too large near the wall, and added a source term S_ε to the right hand side of the transport equation for $\tilde{\varepsilon}$. This term was designed to drive the length scale towards its local equilibrium value, and thereby obtain heat transfer predictions in better agreement with experiment.

$$S_\varepsilon = 0.83\left(\frac{\tilde{\varepsilon}^2}{k}\right)\left(\frac{k^{1.5}}{c_l y\tilde{\varepsilon}} - 1\right)\left(\frac{k^{1.5}}{c_l y\tilde{\varepsilon}}\right)^2 \tag{10}$$

where y is the distance from the wall, and $c_l = 2.5$. As will be discussed later, satisfactory predictions of test data measured by Baughn *et al.* [18] were obtained. This source term was used in all computations reported here.

Boundary conditions

At solid wall, $U_i = k = \tilde{\varepsilon} = 0$, and a constant wall heat flux boundary condition for h is specified. For constant properties the fully developed flow will repeat itself in a succession of cross sections at pitch length L. The approach of Patankar *et al.* [7] was to use periodic boundary conditions, resulting in additional source terms in the momentum and energy equations. In the present study, a simpler approach to the periodic boundary condition has been used. A fixed number of inner iterations were performed for given inlet conditions, and the calculated outlet values of velocities, enthalpy, kinetic energy, and dissipation rates were substituted as inlet conditions for the next

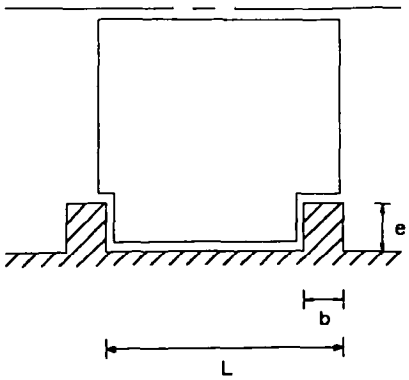

FIG. 2. Schematic diagram of computation cell for flow over rectangular ribs.

outer iteration. A 1/7th power law profile was given for the axial velocity at the inlet for the first outer iteration. The computational domain shown in Fig. 2 was chosen such that the inlet was located at six slabs before the right end of the first rib. Values at slab NX-1 were substituted as the inlet conditions after each outer iteration.

Friction factor and Stanton numbers

The average friction factor is calculated from the pressure drop over one pitch length,

$$f = \frac{\Delta p}{\rho U_b^2 L/D_h}. \tag{11}$$

The local Stanton number is defined as

$$St = \frac{q_w}{\rho U_b c_p (T_w - T_b)} \tag{12}$$

where

$$T_b = \frac{\int_0^H TU \, dy}{\int_0^H U \, dy}. \tag{13}$$

Along the front and rear faces of the ribs, T_b is taken as an average of the values at the upstream and downstream slabs.

An average Stanton number is calculated as

$$St_{av} = \frac{q_w}{\rho U_b c_p (\overline{T_w - T_b})} \tag{14}$$

where the average value of $(T_w - T_b)$ was obtained as

$$\overline{T_w - T_b} = \frac{\int_0^L (T_w - T_b) \, dx}{L} \tag{15}$$

where L is the rib pitch. Use of this definition of St_{av} may give good agreement with average Stanton numbers obtained with a uniform temperature boundary condition, as described by Mills [19]. The average Stanton number including the front and back faces of ribs was also calculated using the entire length of the heated surface for L in equation (15). The difference between the two average St was found to be less than 5% in the present computations. The bulk temperature, T_b, was also calculated from an energy balance, and agreed well with that determined from equation (13).

Thermophysical properties

The assumption of constant fluid properties is not adequate for large heat fluxes into the fluid, since all the physical properties depend on temperature and pressure. Fluid properties for the numerical calculation can be entered as power law approximations. The properties for low-pressure air can be approximated within 4% in the temperature range of about $273 < T < 1500$ K approximated as follows [20]

$$\frac{\mu}{\mu_{in}} = \left(\frac{T}{T_{in}}\right)^{0.67}, \quad \frac{k}{k_{in}} = \left(\frac{T}{T_{in}}\right)^{0.805},$$

$$\frac{c_p}{c_{pin}} = \left(\frac{T}{T_{in}}\right)^{0.095}, \quad \frac{\rho}{\rho_{in}} = \frac{T_{in}}{T}. \tag{16}$$

Due to decrease in density with temperature, there is continuous acceleration of the flow, and also another effect is the increase of the fluid resistance at the wall with heating that causes thickening of the wall boundary layer. These effects must be taken into account in evaluating the wall shear stress. Assuming static pressure is uniform across the flow section and treating the momentum flux as one-dimensional, the wall shear stress becomes

$$\tau_w = -\frac{D}{4} \frac{d(p + \rho U_b^2/2)}{dx}. \tag{17}$$

In the present computation, the friction induced by the momentum change was taken into account in calculating the average friction factor over one pitch length.

The specific heat was taken as a constant, and average viscosity and temperature ratio over the length of a pitch was taken as the average of the inlet and outlet values. A fixed number of inner iterations were performed with a constant wall heat flux boundary condition, and the calculated values of velocities and turbulence quantities at the outlet of the computation domain were substituted as inlet conditions for the next outer iteration.

Numerical procedures

The PHOENICS [21] program developed by CHAM Ltd. has been used in the present study. The program employs a variant of the SIMPLE algorithm [22] called SIMPLEST to solve the hydrodynamic equations. The discretized equations with the hybrid scheme are solved by the TDMA (Tri-Diagonal-Matrix-Algorithm). The low-Reynolds number k–ε model has been implemented in the code with appro-

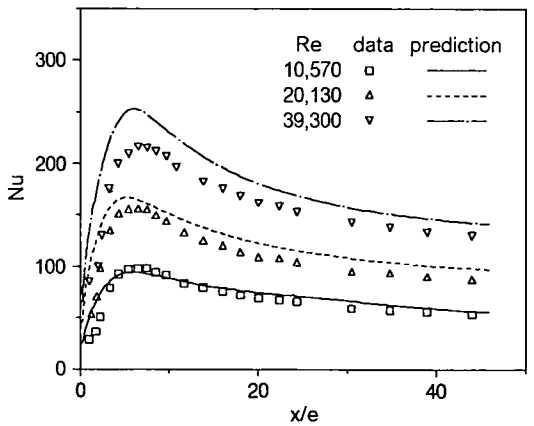

FIG. 3. Comparison of Nusselt number with the data of Baughn *et al.* $d/D = 0.8$.

priate linearization of the source terms. Details may be found in ref. [12].

The criterion of convergence of the numerical solution is based on the absolute normalized residuals of the equations that was summed for all cells in the computation domain. The solutions are regarded as converged when these normalized residuals become less than 10^{-3} for the continuity equation and 10^{-2} for other variables.

In the case of the turbulent flow in a channel with ribs, a typical output had the normalized absolute residuals of $7e-5$, $2e-3$, $1.5e-3$, 0.45, 0.45, $4.4e-3$, for continuity, V momentum, U momentum, k, ε, and energy equation respectively, after 1500 sweeps. In addition to the whole-field residuals, the average friction factor and the average heat transfer coefficient were monitored at every 50 sweeps for the problem of flow in channel with ribs. The relative errors of the average friction factor and the average heat transfer coefficient computed at each outer iteration was less than 1% for all cases studied.

COMPUTATIONAL RESULTS AND DISCUSSION

The low-Reynolds number turbulence model was first tested for flow downstream of an abrupt pipe expansion. The parameters considered were a downstream Reynolds number from 10 570 to 39 300 and $d/D = 0.8$. The inlet conditions were fully developed profiles for all the variables that were obtained at 50 diameters downstream to simulate the experimental

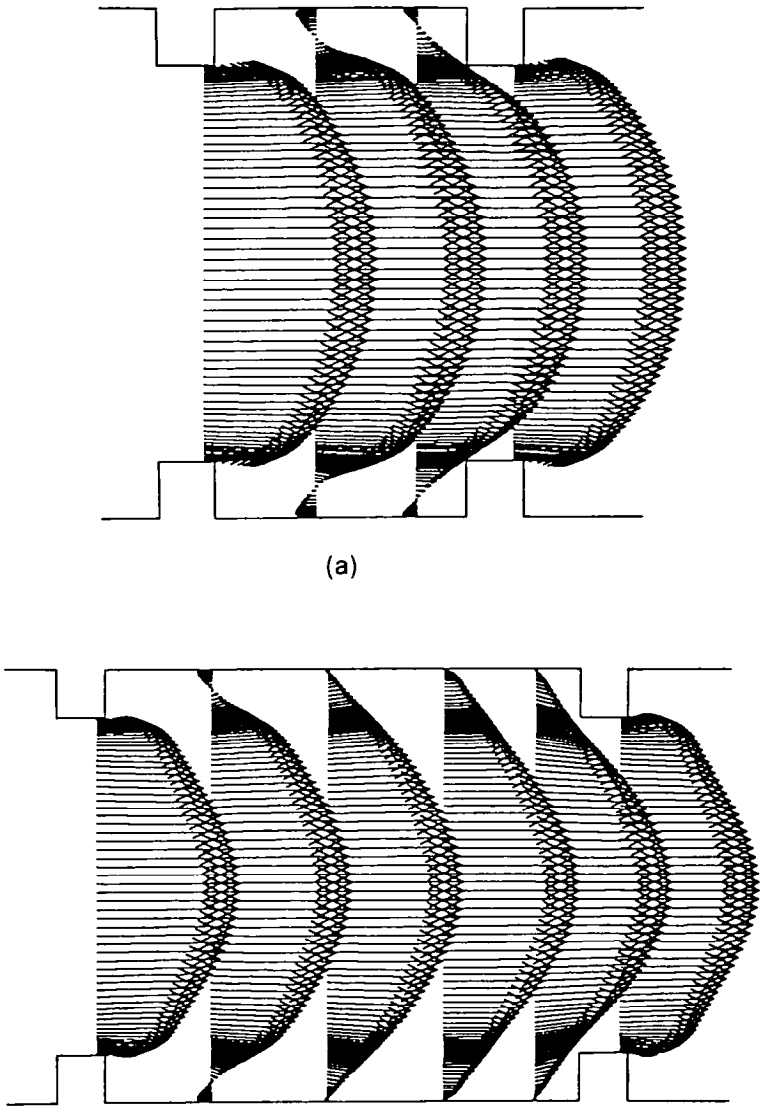

FIG. 4. Velocity plots for flow in a channel with ribs for $Re = 20\,900$. (a) $L/e = 5$, (b) $L/e = 10$.

condition of Baughn *et al.* [18] using wall function boundary conditions, except enthalpy, which was uniform. The outlet was located about 100*e* downstream from the step so that its influence on the main flow would be negligibly small. Air was chosen as the fluid, and properties were evaluated at 293 K. A constant wall heat flux of 700 W m^{-2} was used on the downstream wall, which was in the range of Baughn's experiment. The turbulent Prandtl number was fixed at 0.9. A typical grid used was $NY = 47$ and $NX = 73$ with 57% of the grids located between the wall the the top of the step in the radial direction.

The local Nusselt number distribution for $d/D = 0.8$ and $Re = 10\,570$, 20 130 and 39 300 are shown in Fig. 3. The prediction is fairly good except at high Re, where about 18% overprediction occurs at the reattachment point. When Yap's source term was not included, the prediction for Nu was about 2.1 times higher in the vicinity of the reattachment point for $d/D = 0.8$ and $Re = 20\,130$. It is relevant to note here that both Yap and Amano [23] tested non-equilibrium wall functions with the high Reynolds number k–ε model for this flow, and obtained unsatisfactory results. Based on the results for $d/D = 0.8$, the turbulence model was thought to have sufficient merit to warrant its application to flow over transverse ribs.

Parametric studies for transverse ribs were performed for $e/D = 0.056$, $e/b = 0.67$, and 1, $L/e = 5$, 7.5, 10, 15, 20, and $Re = 5200$–41 800. Air was chosen as the fluid, and properties were evaluated at 293 K. The wall heat flux used was 500 W m^{-2}. A typical grid used for $L/e = 10$ was $NX = 84$ and $NY = 74$ with 60% of the grids located between the wall and the rib top. Figure 4 shows the velocity distribution for $L/e = 5$ and 10 at $Re = 20\,900$. For $L/e = 5$, a large recirculation is present between the ribs and there is no flow reattachment. Though not shown in the figures, a small counterrotating vortex was observed in the corner behind the first rib. The static pressure contours for $L/e = 5$ and 15 are shown in Fig. 5. The turbulent kinetic energy contours in Fig. 6 show maxima at the sharp edge of the second rib where flow impinges and a highly turbulent shear layer is generated. A second maximum occurs upstream of the flow reattachment for $L/e = 10$, which was about 5.6*e* downstream from the edge of the first rib for $Re = 20\,900$.

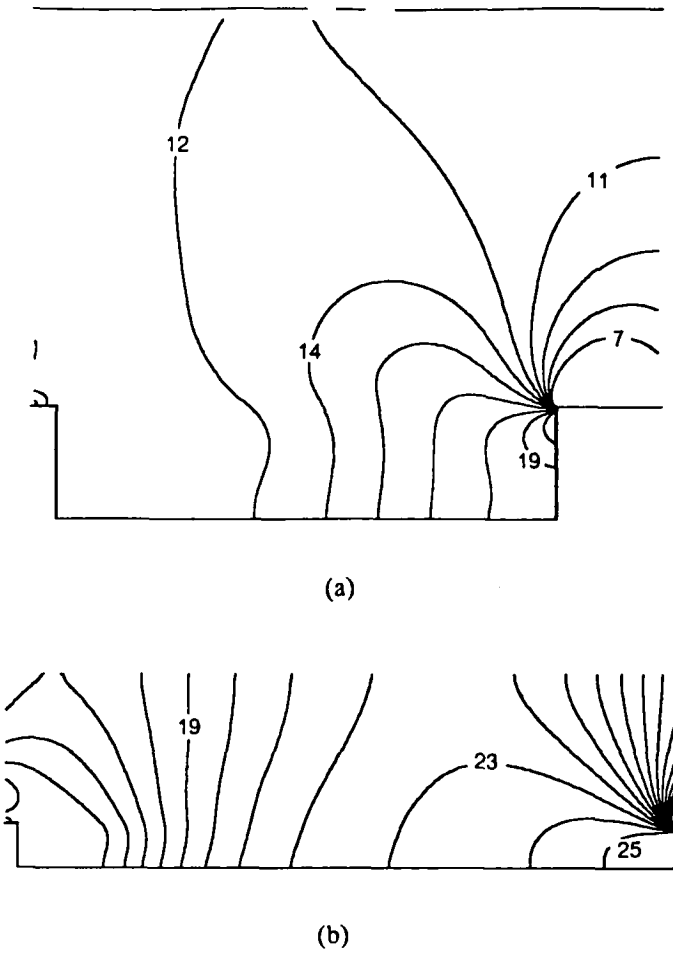

FIG. 5. Static pressure contour for $Re = 20\,900$. (a) $L/e = 5$, (b) $L/e = 15$.

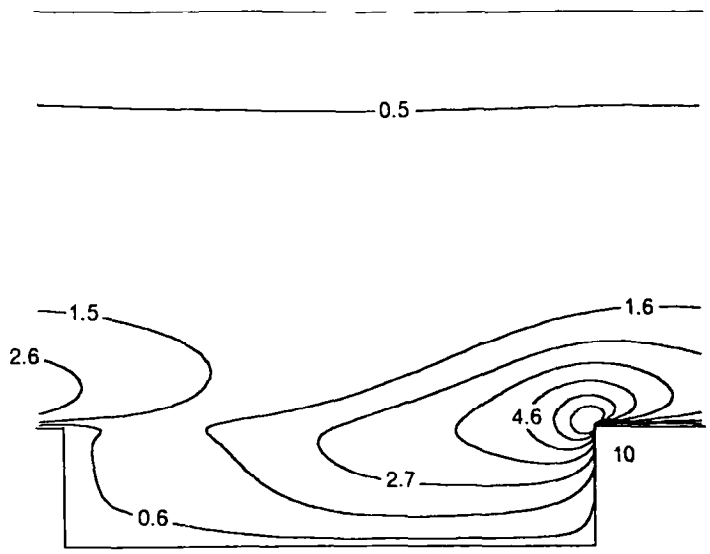

(a)

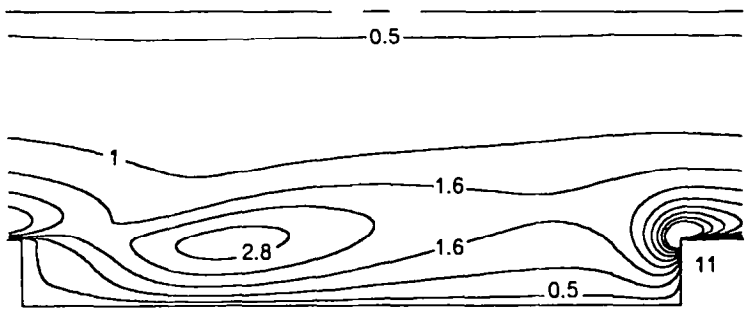

(b)

FIG. 6. Turbulent kinetic energy contour for $Re = 20\,900$. (a) $L/e = 5$, (b) $L/e = 10$.

Isotherms for $L/e = 5$ and 10 in Fig. 7 show high temperature regions where recirculations occur. Figure 8 shows the prediction of temperature and heat transfer rates along the channel wall including the front and back side of the rib for $L/e = 5$ and 10. The region between the first two vertical markers in the figures corresponds to the front side of the rib, and that between the second and third markers corresponds to the top of the rib. The temperature is the lowest at the top of the front side of the rib where there is a flow impingement, and the highest heat transfer coefficient is obtained. The boundary-layer development at the top of the second rib also leads to low wall temperature, and there is a sudden increase in temperature at the back side of the rib. For $L/e = 5$, another maximum in local heat transfer coefficient between the ribs lies close to the second rib where the faster moving fluid above the ribs has penetrated. The temperature and local St distribution along the wall for $L/e = 10$ show the lowest wall temperature and the highest heat transfer coefficient between the ribs about $2e$ upstream of the reattachment point. It appears that the average heat transfer coefficient for $L/e = 5$ and 10 are not very different. In fact, the experimental data of Han *et al.* [24] showed that there is an increase of only about 9% in the average Stanton number when L/e was increased from 5 to 10 at $Re = 13\,500$. The current computation showed an increase of about 11%.

Figure 9 shows a comparison of the average friction factor and Stanton number with the experimental data of Han *et al.* The agreement of the friction factor with experiment is generally good, except for the underprediction of about 10% for both $L/e = 10$ and 15 at Re of about 20 000. For $L/e = 5$ and 7.5, well converged results for $Re < 20\,000$ were difficult to obtain,

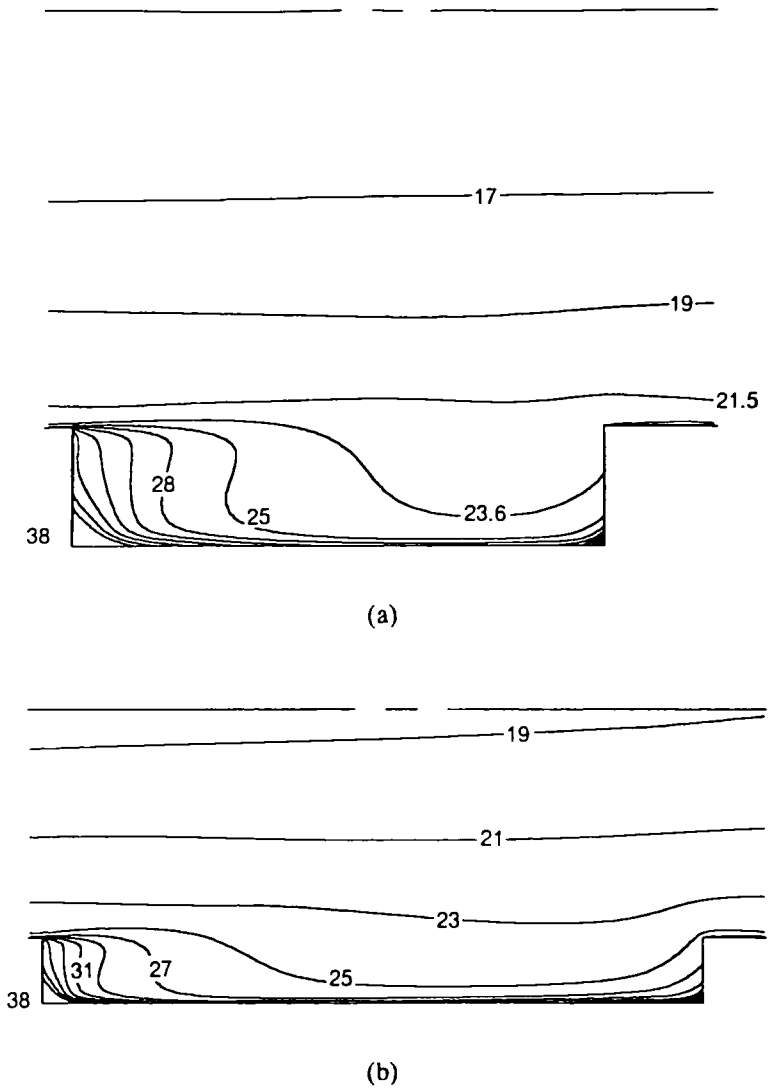

FIG. 7. Isotherms for $Re = 20\,900$. (a) $L/e = 5$, (b) $L/e = 10$.

and they will not be presented. The prediction of the average St shows generally good agreement with experimental data, but the computed values for $L/e = 10$ and 15 are underpredicted by about 17–15% and 18–9% respectively over the range of $Re = 5000$–$20\,000$. The present predictions for the abrupt pipe expansion flow shows the need to correct the extra source term in the ε equation to predict correctly the Reynolds number dependence. The heat transfer prediction is also sensitive to the details of near-wall flow field such as the location and length of reattachment. Higher order models, such as the algebraic stress model and higher order differencing schemes, might give a superior simulation of this complex flow. Figure 10 is a typical plot of local Stanton number along the tube wall after each outer iteration. The total number of outer iterations shown is 20, and gradual convergence is obtained, though the behavior is erratic.

A channel with $L/e = 15$, $e/D = 0.056$ was chosen to observe the effect of variable physical properties. The low-Re model with the Yap modification was employed. The inlet Reynolds number was varied from 11 500 to 20 000, and the calculated temperature ratio, T_w/T_b, varied between 1.42 and 1.88. Pr and c_p were assumed constant for these initial calculations. Iterations were performed until a stabilized value of friction factor and Stanton number were obtained. In the present computation, the calculated variables at the outlet after an outer iteration were substituted as inlet conditions for the next outer iteration. Thus, the temperature level is increasing in the computation domain for successive outer iterations, and the process is very similar to marching in the flow direction. Turbulence intensities should decay towards zero if relaminarization takes place due to heating. A detailed study of relaminarization on the turbulence structure is beyond the scope of the present investigation, but

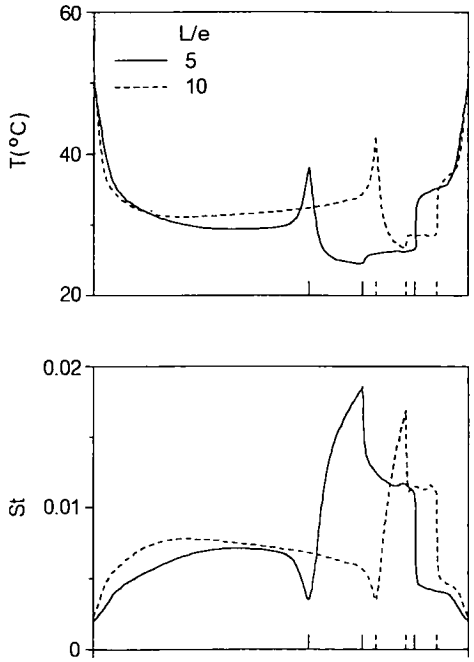

FIG. 8. Prediction of wall temperature and Stanton number for $Re = 20\,900$.

a transition was observed at high heat fluxes. In the neighborhood of the reattachment point, there was an increase of about four-fold in the viscous sublayer

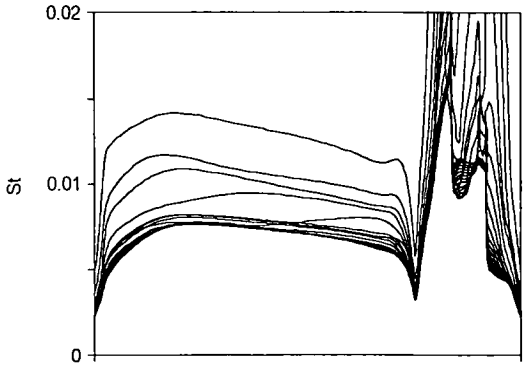

FIG. 10. Local Stanton number distribution with outer iteration. $L/e = 10$, $Re = 20\,900$.

thickness, and the turbulence kinetic energy in the viscous sublayer close to the wall decayed to about 1/4 of that for the constant property flow with the same initial Reynolds number, when the bulk Reynolds number decreased to about 45% of the initial Reynolds number.

Figure 11 shows a plot of f/f_c vs T_w/T_b for $Re = 10\,000$ and 15 000, where f_c is the constant property value. With variable properties it proved difficult to obtain a properly converged solution at $Re = 20\,000$, and thus these results are not included. The Reynolds number is an average value calculated with bulk properties over a pitch. The present calculation shows about 21 and 13% reduction in f at $Re = 10\,000$ and 15 000 respectively when the air was heated to about $T_w/T_b = 1.7$. The results also show an increase in f/f_c with increasing Re and in contrast

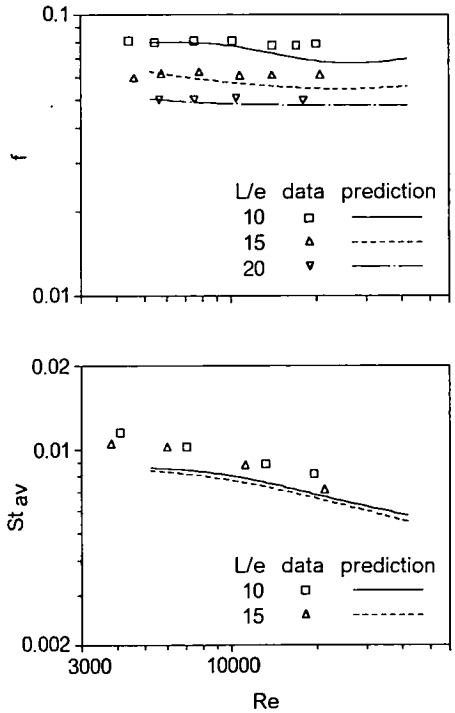

FIG. 9. Comparison of average friction factor and Stanton number with the data of Han *et al.*

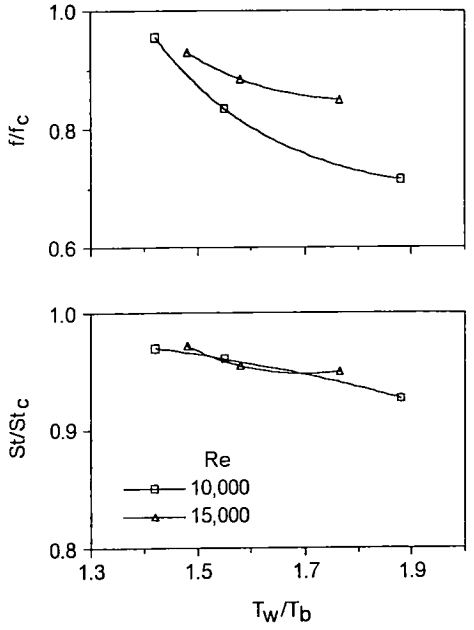

FIG. 11. Normalized friction factor and Stanton number versus temperature ratio for repeated rib roughness. $e/D = 0.056$, $L/e = 15$.

to the constant property situation, the effect of Re on f is not negligible. The experimental data of Vilemas and Simonis [25] showed a large effect of temperature ratio on friction at low range of Re but smaller effect of Re on friction. They found a 20% decrease in f in the Reynolds number range of 10 000 to 20 000 when the channel was heated to $T_w/T_b = 1.8$ from an adiabatic flow condition. The effect of Reynolds number on f was negligible for heating up to $T_w/T_b = 1.8$ in the range of Reynolds number less than about 60 000. However, the data for the influence of temperature ratio on friction is for one channel only ($e/D = 0.013$, $L/e = 9.5$), and the effect of the parameter e/D_h could not be discerned. The friction factor measured in the experiment of Vilemas and Simonis was the overall friction factor with an outer smooth wall and inner rough wall, whereas the present computation is performed with the both walls of identical roughness. Thus an exact comparison cannot be made. The channel of the present computation also has much larger pitch to roughness height ratio than the test section of Vilemas and Simonis, and the ratio of the roughness height to the channel height of flow passage is about 11% compared to only 2.6% in the experiment. Thus, the channel of the present study has larger flow recirculation and redeveloped regions than the experimental setup.

Figure 11 also shows the plot of St/St_c vs T_w/T_b. There is about 5% reduction in heat transfer rate for both $Re = 10\,000$ and 15 000 when the air is heated to $T_w/T_b \simeq 1.7$. There is no apparent effect of Reynolds number on heat transfer for the small range of Reynolds number in the present computation. This seems to be supported by the experimental results of Vilemas and Simonis, which show only about 5% difference in Nu/Nu_c from $Re = 11\,000$ to 31 000 when the air was heated to $T_w/T_b \simeq 1.7$. However, their results show a much higher reduction in heat transfer with heating in the low Reynolds number range: about 19% at $Re = 11\,000$ when the gas was heated to $T_w/T_b \simeq 1.7$. More computations need to be performed in order to investigate the effect of Reynolds number and the parameter e/D_h.

CONCLUSIONS

The low-Reynolds number turbulence model of Jones and Launder gave fairly good results for both the abrupt pipe expansion flow and flow in a channel with repeated rectangular ribs. Predictions for heat transfer were generally poorer than that for friction factor for the repeated ribs. Further modifications to ε-equation or to the extra source term is needed to predict correctly the Reynolds number dependence of the heat transfer. The effect of variable properties in the Reynolds number range of present study was greater for the friction than for heat transfer. Further parametric studies are needed.

Acknowledgements—This work was funded by the National Aeronautics and Space Administration Ames-Dryden Flight Research Facility through the U.C.L.A. Laboratory for Flight Systems Research, director, Professor A. V. Balakrishnan. The NASA Technical Officer was Mr R. D. Quinn, and the funding was facilitated by Dr K. Illif of NASA Dryden.

REFERENCES

1. K. Maubach, Rough annulus pressure drop-interpretation of experiments and recalculation for square ribs, *Int. J. Heat Mass Transfer* **15**, 2489–2498 (1972).
2. M. Dalle Donne and L. Meyer, Turbulent convective heat transfer from rough surfaces with two-dimensional rectangular ribs, *Int. J. Heat Mass Transfer* **20**, 583–620 (1977).
3. J. R. Taylor, Heat transfer phenomena in gas turbine, ASME Paper No. 80-GT-172 (1980).
4. J. C. Han, Heat transfer enhancement in channels with turbulence promoters, *J. Engng for Gas Turbines and Power* **107**, 628–635 (1985).
5. M. J. Lewis, An elementary analysis for predicting the momentum and heat transfer characteristics of a hydraulically rough surface, *J. Heat Transfer* **97**, 249–254 (1975).
6. B. K. Lee, N. H. Cho and Y. D. Choi, Analysis of periodically fully developed turbulent flow and heat transfer by k–ε equation model in artificially roughened annulus, *Int. J. Heat Mass Transfer* **31**, 1797–1806 (1988).
7. S. V. Patankar, C. H. Liu and E. M. Sparrow, Fully developed flow and heat transfer in ducts having streamwise-periodic variations of cross-sectional area, *J. Heat Transfer* **99**, 180–186 (1977).
8. M. A. Leschziner and W. Rodi, Calculation of annular and twin parallel jet using various discretization schemes and turbulence-model variations, *J. Fluid Engng* **103**, 352–360 (1981).
9. T. M. Liou, D. C. Hwang and C. F. Kao, Computations of turbulent flow and heat transfer enhancement in channel with a pair of turbulence promoters, *3rd International Symposium on Transport Phenomena in Thermal Control*, Taipei, Taiwan (1988).
10. F. Durst, M. Founti and S. Obi, Experimental and computational investigation of the two-dimensional channel flow over two fences in tandem, *J. Fluid Engng* **110**, 48–54 (1988).
11. T. M. Liou, Y. Chang and D. W. Hwang, Experimental and computational study of torbulent flows in a channel with two pairs of turbulence promoters in tandem, *J. Fluid Engng* **112**, 302–310 (1990).
12. B. H. Chang and A. F. Mills, Application of a low-Reynolds number turbulence model for a tube with repeated roughness, *Proceedings of 4th International PHOENICS User Conference*, Miami, Florida, 262–288, April 15–19 (1991).
13. C. Yap, Turbulent heat and momentum transfer in recirculating and impinging flows, Ph.D. Thesis, Faculty of Technology, University of Manchester, U.K. (1987).
14. W. P. Jones and B. E. Launder, The calculation of low-Reynolds number phenomena with a two-equation model of turbulence, *Int. J. Heat Mass Transfer* **16**, 1119–1130 (1972).
15. M. Ciofalo and M. W. Collins, k–ε predictions of heat transfer in turbulent recirculating flows using an improved wall treatment, *Numerical Heat Transfer* **15**, Part B, 21–47 (1989).
16. T. Cebeci and P. Bradshaw, *Physical and Computational Aspects of Convective Heat Transfer*. Springer-Verlag, New York (1984).
17. B. E. Launder and B. I. Sharma, Application of the energy-dissipation model of turbulence to the calculation

of flow near a spinning disc, *Letters in Heat Mass Transfer* **1,** 131–138 (1974).
18. J. W. Baughn, M. A. Hoffman, R. K. Takahashi and B. E. Launder, Local heat transfer downstream of abrupt expansion in a circular channel with constant wall heat flux, *J. Heat Transfer* **106,** 789–796 (1984).
19. A. F. Mills, Average Nusselt numbers for external flows, *J. Heat Transfer* **101,** 734–735 (1979).
20. D. M. McEligot, S. B. Smith and C. A. Bankston, Quasi-developed turbulent pipe flow with heat transfer, *J. Heat Transfer* **92,** 641–650 (1970).
21. H. I. Rosten and D. B. Spalding, *The PHOENICS beginner's guides*, CHAM report no. TR100, CHAM Limited, Bakery House, 40 High Street, Wimbledon SW19 5AU England (1986).
22. S. V. Patankar and D. B. Spalding, A calculation procedure for heat mass and momentum transfer in three-dimensional parabolic flows, *Int. J. Heat Mass Transfer* **15,** 1778–1806 (1972).
23. R. S. Amano, Development of a turbulence near-wall model and its application to separated and reattached flows, *Numerical Heat Transfer* **7,** 59–75 (1984).
24. J. C. Han, L. R. Glicksman and W. M. Rohsenow, An investigation of heat transfer and friction for rib-roughened surfaces, *Int. J. Heat Mass Transfer* **21,** 1143–1156 (1978).
25. J. V. Vilemas and V. M. Simonis, Heat transfer and friction of rough ducts carrying gas flow with variable physical properties, *Int. J. Heat Mass Transfer* **28,** 59–68 (1985).